ANALYSIS OF MULTI-BUNCH INSTABILITIES AT THE DIAMOND STORAGE RING

R. Bartolini[1], R. Fielder, G. Rehm, Diamond Light Source, Oxfordshire, UK
V. Smaluk, NSLS II, Brookhaven National Laboratory, USA
[1]also at John Adams Institue, University of Oxford, UK

Abstract

We present the result of the analytical, numerical and experimental analysis of multi-bunch instabilities at the Diamond storage ring. This work compares the impedance estimates with CST with the analysis of the growth rates of the excited multi-bunch modes in different machine configurations. The contribution of a number of wakefield sources has been identified with very high precision thanks to high quality data provided by the existing TMBF diagnostics.

INTRODUCTION

Multibunch collective effects can be a source instability that reduce the performance of third generation light sources like Diamond. They are driven by long range wakefields, usually trapped modes in cavity-like structures in the vacuum vessel, or resistive wall (RW) impedances [1]. While the use of superconducting cavities intrinsically reduces the impact of high order modes (HOMs), Diamond still suffers from RW and occasionally from multibunch ion instabilities. A transverse multibunch feedback system (TMBF) was installed in 2008 [2] and has proven to be very effective in damping all coupled bunch modes, at the operating current (300 mA) in full fill (936 bunches) at zero chromaticity. The TMBF system provides a wealth of data that can be used to characterise the impedance of the machine, validate the impedance model and simulations of beam dynamics [3]. In this paper we present the results of a campaign of measurements and analysis made at Diamond in the last two years.

THEORY

Transverse Multibunch Oscillations

In a multi-bunch train without wakefields all bunches evolve independently. Each bunch oscillates with the betatron frequency $\omega_{x,y}$. The motion of the bunch train can be expanded in Fourier modes, (M bunches = M modes, and in a full fill, M = harmonic number). However, without wakefields there is no reason to prefer this set to any other "basis" (i.e. modes are degenerate).

When bunches are coupled by wakefields, each bunch oscillates with the betatron frequency $\Omega_{x,y}$. In the limit of small wakefields the Fourier modes are eigenvectors of the time evolution, i.e. modes are preserved during the time evolution. The betatron oscillation frequency becomes complex, i.e. $\mathrm{Im}(\Omega) \propto \mathrm{Re}Z$ describes the damping or anti-damping and $\mathrm{Re}(\Omega) \propto \mathrm{Im}Z$ describes the frequency shift. The degeneracy of the Fourier modes is broken, i.e. $\Omega = \Omega(\mu)$.

Complex frequency shift and driving impedance

For M bunches with finite length and internal modes, the complex frequency shift of the mode(μ, l) is [1]:

$$\Omega^{(\mu,l)} - \omega_\beta = -i\frac{MNr_0c}{2\gamma T_0^2\omega_\beta}\sum_{p=-\infty}^{\infty} Z_1^\perp(\omega_{\mu,l})\cdot h_l(\omega_{\mu,l})$$

where ω_β is the unperturbed betatron frequency, N is the number of particles per bunch, r_0 is the classical radius of the particle, γ is the Lorentz factor, T_0 is the revolution period, $Z_1^\perp$is the transversedipole impedance, h_l is the bunch mode spectral power. Mode (μ, l) is driven by the impedance sampled at the discrete set of frequencies:

$$\omega_{\mu,l} = (pM + \mu)\omega_0 + \omega_\beta + l\omega_s \ ,$$

where ω_s is the synchrotron frequency.

With non-zero chromaticity ξ, the complex frequency shift is given by:

$$\Omega^{(\mu,l)} - \omega_\beta = -i\frac{MNr_0c}{2\gamma T_0^2\omega_\beta}\sum_{p=-\infty}^{\infty} Z_1^\perp(\omega_{\mu,l})\cdot h_l(\omega_{\mu,l} - \omega_\xi)$$

Here, the bunch samples the impedance at $\omega_{\mu,l}$ but the bunch frequency spectrum is shifted at $\omega_{\mu,l} - \omega_\xi$, where $\omega_\xi = \xi\omega_\beta/\eta$, $\eta = \alpha - \gamma^{-2}$, and α is the momentum compaction factor. The coherent frequency shift and growth rate are $\mathrm{Re}\Omega^{(\mu,l)} - \omega_\beta$ and $\mathrm{Im}\Omega^{(\mu,l)}$, respectively.

Sampling in Time and Aliasing in Frequency

A mode μ sampled turn-by-turn corresponds to the frequency $\mathrm{frac}(\Omega_{x,y})$ aliased in $[0, \omega_0] \rightarrow \mathrm{frac}(\Omega_{x,y})$ i.e. fractional part of the tune.A mode μ sampled bunch-by-bunch corresponds to the frequency $\mu\omega_0 + \Omega_{x,y}$aliased in $[0, M\omega_0]$, i.e. baseband of the RF. For a real signal the spectrum is further folded symmetrically in $[0, M\omega_0/2]$.

GROW-DAMP EXPERIMENTS

Grow-damp measurements are done in three steps: artificially excite mode μ by using a stripline driven at the frequency $(pM + \mu)\omega_0 + \omega_\beta$; stop the excitation and measure free oscillations (damped or anti-damped); run feedback to damp any unstable mode or residual oscillation. This is repeated for all modes μ = 0, 1, ..., M - 1.

Diamond Storage Ring Parameters

In the Diamond storage ring there are M=936 bunches, giving a 2 ns (500 MHz) repetition rate at full fill and a 530 kHz revolution frequency. The maximum current is 300 mA, and the bunch length 15-25 ps rms. The beam is

ISBN 978-3-95450-147-2

excited at mode μ for 250 turns, then the excitation is stopped and free oscillations are measured for some turns, typically 250-2000 (see Fig. 1). Since it is very slow to transfer all bunch-by-bunch data, only the Fourier component (amplitude and phase) at the frequency of interest for mode μ is stored. This reduces the data transfer from 1.3 GB to 5.6 MB [2]. Offline post-processing gives the frequency shift and damping or growth rate.

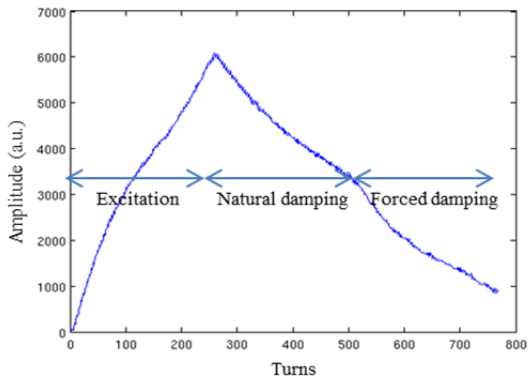

Figure 1: grow-damp measurement recording the turn-by-turn amplitude of the mode previously excited.

Vertical Growth Rates

Figure 2 shows an example of fitted damping rates for all 936 modes. These data suggest that the impedance is largely dominated by resistive wall, with a small number of high Q resonators. The resistive wall component can be calculated by Eq. 1, using the average values of β function β = 12.25m, half-height of the vacuum chamber b = 13.5mm and resistivity ρ = 7.3*10^{-7}Ωm for the Diamond storage ring.

$$\frac{Z^{rw}_{x,y}}{L} = G_{lx,y}\,\frac{sgn(\omega)+i}{\pi b^3}\sqrt{\frac{Z_0 c\rho}{2}}\,|\omega|^{-1/2} \qquad (1)$$

Here $G_{lx,y}$ is the form-factor for the elliptic cross-section of vacuum chamber.

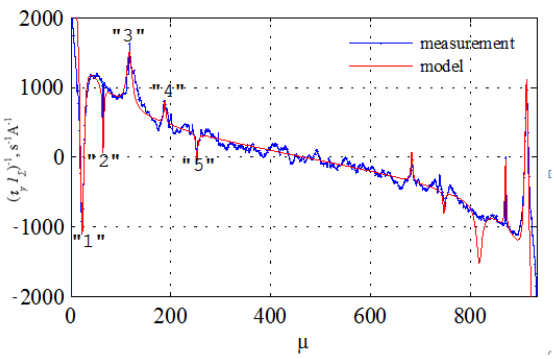

Figure 2: Vertical damping rates normalised by the beam current for all 936 modes after subtraction of radiation damping (measured data in blue, fit in red).

Five main separate resonators are identified and their parameters fitted using equation 2.

$$Z_{\perp}^{res} = \frac{R_S}{\frac{\omega}{\omega_r}+iQ\left(\frac{\omega^2}{\omega_r^2}-1\right)} \qquad (2)$$

Two of these ("3" and "4" shown in Fig. 2) can be attributed to the in-vacuum insertion devices (IDs), of which there are 14 in the Diamond storage ring. IDs installed in phase one and phase two of the Diamond project are observed to have different behaviour due to differences in design, primarily in the tapers at each end of the ID. Fig. 3 shows the effect of ID gaps closing on the damping rates including both geometric impedance and ID contribution to the resistive wall impedance.

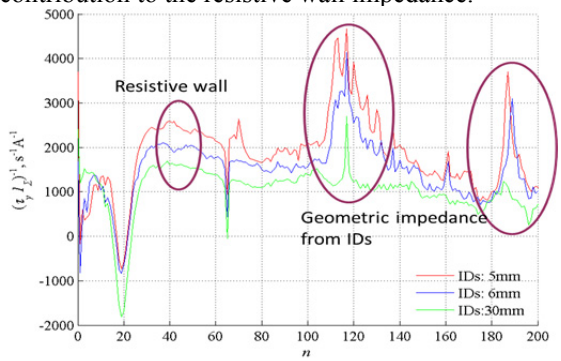

Figure 3: Effect on vertical damping rates of closing all in-vacuum IDs.

Three other peaks ("1", "2", and "5") can be likely attributed to the beam position monitors (BPMs), of which there are 175 in the storage ring. Fig. 4 shows the longitudinal impedance of all the BPMs obtained from CST simulations, and the transverse impedance resulted from the fit of measured rates. The parameters of the resonators are summarized in Table 1. Of course, we cannot compare the longitudinal and transverse impedances directly but the resonant frequencies look close to each other, however the shunt impedances and quality factors do not fit well. The resonators fitted are shown in Table 1, and plotted with the simulated BPM impedance in Fig. 4.

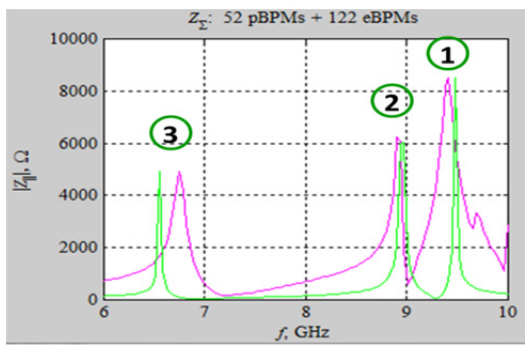

Figure 4: Sum of vertical impedance from CST simulation for all BPMs (pink) with fit of resonators (green).

Table 1: Parameters of Fitted Resonators

Peak	Resonant mode	f_r (GHz)	R_s (MΩ/m)	Q
1	19M–22	9.4813	4.4	2,000
2	18M – 64	8.9593	1.4	5,000
5	13M – 253	6.8603	0.5	3,000

Simulations

Simulations for a range of components in the Diamond ring were conducted using the wakefield solver in CST Particle Studio. By summing the impedances found, a

total impedance spectrum could be calculated and the most significant contributors identified. While some individual components have relatively large impedance, it was found that the BPMs appeared to be the most significant due to their sharp peaks indicating high-Q resonances combined with the large number in the ring.

FURTHER MEASUREMENTS

Collimator

The largest peak in damping rates, initially at mode 22, was observed to have moved over the course of several months, indicating that fixed components such as BPMs could not be the cause for such peaks. Experiments identified the vertical collimator as the culprit (Fig. 5), where a sticking motor had resulted in an offset to the expected gap. This had not been predicted since the original simulations for this component had been conducted on a greatly simplified model using the old MAFIA wakefield code. Further simulations in CST Studio identify a large peak in impedance for this collimator at ~1.5GHz, which agrees well with the observed peak in measurements. This is due to the gap around the collimator block forming a cavity nominally 1mm wide which changes in depth as the block is moved. A campaign of simulations considering manufacturing tolerances and possible damage to RF fingers is ongoing.

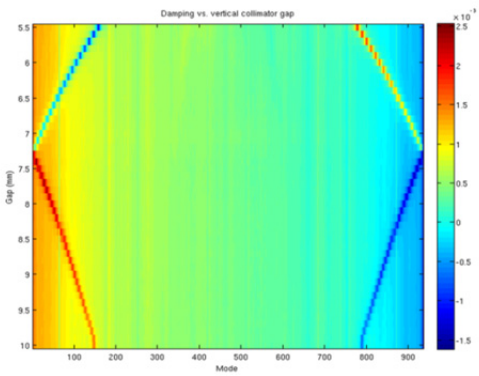

Figure 5: Measured damping rate vs. vertical collimator gap.

Insertion Devices

More detailed measurements of the effects of individual IDs have been carried out, moving the IDs in steps of a few microns. These experiments have shown that there is not simply a continuous shift in the frequency of impedance peaks, but also occasional sharp steps (Fig. 6). Unfortunately it is currently impractical to model these structures in the detail required. It is suspected that these jumps are the result of mechanical movements which could not be easily modelled by wakefield software.

Other Measurements

A suite of other experiments continues to be carried out to investigate the effects of various machine parameters on the impedance and effects of impedance on the beam. These include different RF voltages, which result in different bunch lengths and therefore a different sampling of the impedance spectrum (Fig. 7), and chromaticity, adding the coherent damping term to the damping rate measurements.

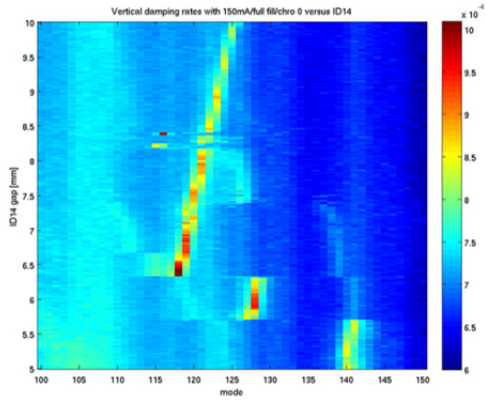

Figure 6: Damping rate vs. gap of I14 in-vacuum ID.

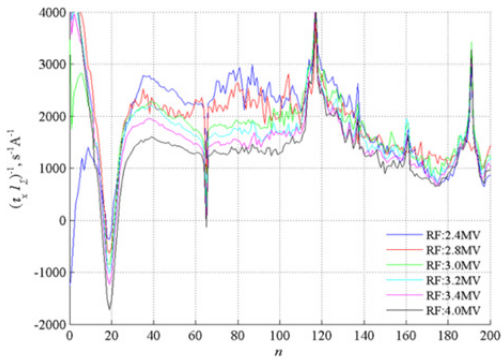

Figure 7: Vertical damping rates vs. RF voltage.

CONCLUSIONS

The Diamond TMBF system allows extensive and repetitive grow damp measurements allowing parameter scans and a regular monitoring of the impedance of the machine. Although all coupled bunch modes are stabilised by the TMBF system, it is clear that the machine impedance is complicated and changing with time in way that is difficult to interpret and predict. More quantitative evaluation of the impedance and investigation of the specific resonances and their causes is ongoing.

ACKNOWLEDGMENTS

The authors would like to thank Alun Morgan and the Diamond Diagnostics group for their help with the TMBF system.

REFERENCES

[1] A. W. Chao, “Physics of Collective Beam Instabilities in High Energy Accelerators”, New York, USA: Wiley, 1993.
[2] G. Rehm *et al.*, in *Proc. IBIC’14*, paper WEPD24.
[3] E. Koukovin-Platia *et al.*, “Single Bunch Instability Studies at Diamond Light Source”, presented at IPAC’16, Busan, Korea, May 2016, paper MOPOR018.

ISBN 978-3-95450-147-2